J|A|C|S
ARTICLES
Published on Web 04/12/2002

A Density Functional Theory Study on the Active Center of Fe-Only Hydrogenase: Characterization and Electronic Structure of the Redox States

Zhi-Pan Liu and P. Hu*

Contribution from the School of Chemistry, The Queen's University of Belfast, Belfast, BT9 5AG, U.K.

Received August 1, 2001. Revised Manuscript Received October 12, 2001

Abstract: We have carried out extensive density functional theory (DFT) calculations for possible redox states of the active center in Fe-only hydrogenases. The active center is modeled by $[(H(CH_3)S)(CO)(CN^-)Fe^p(\mu\text{-DTN})(\mu\text{-CO})Fe^d(CO)(CN^-)(L)]^z$ (z is the net charge in the complex; Fe^p = the proximal Fe, Fe^d = the distal Fe, DTN = ($-SCH_2NHCH_2S-$), L is the ligand that bonds with the Fe^d at the trans position to the bridging CO). Structures of possible redox states are optimized, and CO stretching frequencies are calculated. By a detailed comparison of all the calculated structures and the vibrational frequencies with the available experimental data, we find that (i) the fully oxidized, inactive state is an Fe(II)−Fe(II) state with a hydroxyl (OH^-) group bonded at the Fe^d, (ii) the oxidized, active state is an Fe(II)−Fe(I) complex which is consistent with the assignment of Cao and Hall (*J. Am. Chem. Soc.* **2001**, *123*, 3734), and (iii) the fully reduced state is a mixture with the major component being a protonated Fe(I)−Fe(I) complex and the other component being its self-arranged form, Fe(II)−Fe(II) hydride. Our calculations also show that the exogenous CO can strongly bond with the Fe(II)−Fe(I) species, but cannot bond with the Fe(I)−Fe(I) complex. This result is consistent with experiments that CO tends to inhibit the oxidized, active state, but not the fully reduced state. The electronic structures of all the redox states have been analyzed. It is found that a frontier orbital which is a mixing state between the e_g of Fe and the 2π of the bridging CO plays a key role concerning the reactivity of Fe-only hydrogenases: (i) it is unoccupied in the fully oxidized, inactive state, half-occupied in the oxidized, active state, and fully occupied in the fully reduced state; (ii) the $e_g-2\pi$ orbital is a bonding state, and this is the key reason for stability of the low oxidation states, such as Fe(I)−Fe(I) complexes; and (iii) in the $e_g-2\pi$ orbital more charge accumulates between the bridging CO and the Fe^d than between the bridging CO and the Fe^p, and the occupation increase in this orbital will enhance the bonding between the bridging CO and the Fe^d, leading to the bridging-CO shift toward the Fe^d.

1. Introduction

Hydrogen metabolism ($H_2 \leftrightarrow 2H^+ + 2e^-$) constitutes a central process in the global biological energy cycle, which is mostly mediated by two types of metal-containing enzymes, NiFe hydrogenases[1−3] and Fe-only hydrogenases.[4−9] Of these two forms, the Fe-only hydrogenases are normally found in H_2-producing microorganisms, and its reactivity is generally 1 or 2 orders of magnitude higher than that of their NiFe counterparts.[4−9] In the last 30 years, the high reactivity of Fe-only hydrogenases has stimulated many experimental studies to focus on their structures[10,11] and redox properties.[12−16] To date, much progress has been made. However, some important issues remain to be investigated to fully understand the catalytic mechanism of Fe-only hydrogenases. In particular, study on the electronic structure of the active center of Fe-only hydrogenases has been limited. In this contribution, we present a detailed theoretical characterization of the redox states of the active center in Fe-only hydrogenases, aiming to provide insight into the high catalytic ability of Fe-only hydrogenases.

A breakthrough in the study of Fe-only hydrogenases was made when X-ray crystal structures of two types of Fe-only hydrogenases, CpI (*Clostridium pasteurianum*)[10] and DdH

* To whom correspondence should be addressed. E-mail: P.Hu@qub.ac.uk.

(1) Albracht, S. P. J. *Biochim. Biophys. Acta* **1994**, *1178*, 167.
(2) Graf, E. G.; Thauer, R. K. *FEBS Lett.* **1981**, *136*, 165.
(3) Volbeda, A.; Charon, M. H.; Piras, C.; Hatchikian, E. C.; Frey, M.; Frontecilla-Camps, J. C. *Nature* **1995**, *373*, 580.
(4) Adams, M. W. W. *Biochim. Biophys. Acta* **1990**, *1020*, 115.
(5) Pryzbyla, A. E.; Robbins, J.; Menon, N.; Peck, H. D. *FEMS Microbiol. Rev.* **1992**, *88*, 109.
(6) Cammack, R. *Nature* **1999**, *397*, 214.
(7) Adams, M. W. W., Mortenson, L. E.; Chen J. S. *Biochim Biophys Acta* **1981**, *594*, 105.
(8) Nicolet, Y.; Lemon, B. J.; Fontecilla-Camps, J. C.; Peters, J. W. *Trends Biochem. Sci.* **2000**, *25*, 138.
(9) Peters, J. W. *Curr. Opin. Struct. Biol.* **1999**, *9*, 670.
(10) Peters, J. W.; Lanzilotta, W. N.; Lemon, B. J.; Seefeldt, L. C. *Science* **1998**, *282*, 1853.
(11) Nicolet, Y.; Piras, C.; Legrand, P.; Hatchikian, E. C.; Fontecilla-Camps, J. C. *Structure* **1999**, *7*, 13.
(12) Patil, D. S.; Moura, J. J. G.; He, S. H.; Teixeira, M.; Prickril, B. C.; Der Vartanian, D. V.; Peck, H. D., Jr.; Legall, J.; Huyanh, B, H. *J. Biol. Chem.* **1988**, *263*, 18732.
(13) Pierik, A. J.; Hagen, W. R.; Redeker, J. S.; Wolbert, R. B. G.; Boersma, M.; Verhagen, M. F. J. M.; Grandee, H, J.; Veeger, C.; Mutsaers, P. H. E.; Sands, R. H.; Dunhan, W. R. *Eur. J. Biochem.* **1992**, *209*, 63.
(14) Hatchikian, E. C.; Forget, N.; Fernandez, V. M.; Williams, R.; Cammack, R. *Eur. J. Biochem.* **1992**, *209*, 357.
(15) Pierik, A. J.; Hulstein, M.; Hagen, W. R.; Albracht, S. P. *Eur. J. Biochem.* **1998**, *258*, 572.
(16) Popescu, C. V.; Munck E. *J. Am. Chem. Soc.* **1999**, *121*, 7877.

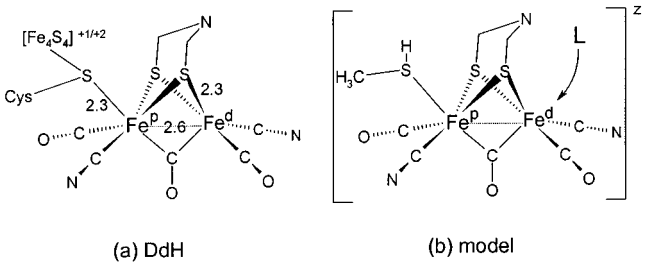

Figure 1. Illustration of **(a)** active center of Fe-only hydrogenases as determined experimentally from *D. desulfuricans*; **(b)** our calculation model used in this work

(*Desulfovibrio desulfuricans*)[11] were reported. The structures of CpI and DdH were found to be closely related;[9] both contain an uncommon six-Fe cluster (H-cluster), which consists of a novel 2Fe subunit cysteine-S bridged to a regular [4Fe−4S] cubane, shown in Figure 1(a). In the 2Fe subunit, the two Fe ions are linked by two bridging thiolate groups and are terminated by CO and CN^- ligands, which is very special in a protein-associated metal cluster because of the toxicity of these ligands as free entities. The two Fe ions are further bridged by a third group: it is a CO in CpI and was tentatively assigned to be an asymmetrically bonded H_2O in DdH initially (for more details, see ref 9).

With respect to the oxidation states of the H-cluster, four redox states were observed, and three of them were well-characterized by a variety of experimental techniques.[11−13] In particular, the FTIR spectra of these three redox states for the H-cluster from *D. vulgaris* were first investigated by Pierik et al.,[15] and the results were found to be insightful with respect to the relationship between the geometrical structure and the redox state in the H-cluster. When the enzyme is isolated in air, the H-cluster is in an *oxidized, inactive state* ($\mathbf{H_{ox}^{air}}$), which is EPR-silent. The $\mathbf{H_{ox}^{air}}$ exhibits three clear CO IR bands from 2050 to 1800 cm^{-1}, of which the lowest band at 1847 cm^{-1} was suggested to be the evidence of a bridging CO (CO_b) in the H-cluster. During the reductive treatment of the as-isolated enzyme, a transient 2.06 rhombic signal was detected by EPR, which was assigned to be a partially reduced and inactive state. Further reductive treatment results in *an oxidized, active state* ($\mathbf{H_{ox}}$), which shows a characteristic band at 1940 cm^{-1} in the FTIR spectrum. The $\mathbf{H_{ox}}$ is a low-spin state with a rhombic $g = 2.10$ signal in EPR. When the Fe-only hydrogenase is fully reduced, another EPR-silent state ($\mathbf{H_{red}}$) is obtained. The FTIR spectrum of the fully reduced state, the $\mathbf{H_{red}}$, is dominated by a high-intensity band at 1894 cm^{-1}, with several other minor peaks.

Very recently, some further important advances were made experimentally. De Lacey et al.[17] obtained high quality FTIR spectra for the $\mathbf{H_{ox}}$ and the CO-inhibited $\mathbf{H_{ox}}$ ($\mathbf{H_{ox}-CO}$) from DdH. Importantly, a low-frequency band at 1802 cm^{-1} was for the first time observed in the $\mathbf{H_{ox}}$, and this band was assigned to be the stretching mode of the CO_b. This finding indicates that the $\mathbf{H_{ox}}$ and the $\mathbf{H_{ox}^{air}}$ have similar structures, such as the existence of a CO_b. Nicolet et al. refined the structure of the $\mathbf{H_{red}}$ from DdH.[18] First, they found that the third ligand that bridges two Fe ions in DdH is, in fact, also a CO ligand, similar to that of CpI. Upon reduction, this bridging CO ligand shifts toward the distal Fe (Fe^d, with respect to the [4Fe−4S] cluster), which is accompanied by a large increase of its stretching frequency. Second, they suggested that the two thioloate groups bridging two Fe ions may be a di(thiomethyl)amine (DTN, $-SCH_2NHCH_2S-$) five-atom chain instead of a PDT chain ($-S(CH_2)_3S-$) speculated initially. This suggestion affords a new proton-transfer channel for the reversible H_2 oxidation reaction on the 2Fe subunit: The N in the DTN, being a base, may attract a proton after H_2 heterolytic cleavage[19] and afterward release this proton to nearby proteins.

While this report was being prepared, two important theoretical studies[20,21] were published by Hall and co-workers. Cao and Hall[20] carried out extensive density functional theory (DFT) calculations on the 2Fe subunit using a (μ-PDT) diiron complex; various redox states, such as Fe(III)−Fe(III), Fe(II)−Fe(II), Fe(II)−Fe(I), and Fe(I)−Fe(I) complexes were calculated, geometrical structures were optimized, and vibrational frequencies of CO and CN^- were obtained. By a detailed comparison between the calculated redox states and the experimental ones, some possible candidates for the $\mathbf{H_{ox}^{air}}$, $\mathbf{H_{ox}}$, and $\mathbf{H_{red}}$ were suggested. They concluded that a reaction cycle involving Fe(II)−Fe(II)↔Fe(II)−Fe(I)↔Fe(I)−Fe(I) is most likely, rather than one with Fe(III)−Fe(III)↔Fe(III)−Fe(II)↔Fe(II)−Fe(II) which was speculated before.[11,16] A step beyond this work, Fan and Hall[21] reported a low-energy route for the H_2 heterolytic cleavage.

Despite these advances, the understanding of the H-cluster in Fe-only hydrogenases is still short of one's expectations. Although Hall and co-workers have calculated a range of possible redox states of the 2Fe subunit, theoretical characterization of these redox states is still not complet, partially because their work was submitted before some important experimental findings were published. For example, the new band at 1802 cm^{-1} ($\upsilon(CO_b)$) observed recently[17] for the $\mathbf{H_{ox}}$ was not identified theoretically.[20−22] Nicolet et al. showed that in the $\mathbf{H_{red}}$ the CO_b shifts toward the Fe^d, being at a bridge-to-terminal position.[18] This structural feature was also not confirmed by theoretical work.[20−22] Because the $\mathbf{H_{ox}^{air}}$, $\mathbf{H_{ox}}$ and $\mathbf{H_{red}}$ are the important intermediates in the catalytic H_2 evolution, further theoretical studies of these redox states are required. In this study, we have carried out a detailed theoretical characterization on the redox states of the 2Fe subunit in Fe-only hydrogenases, using DFT with a plane wave basis set. It has been demonstrated that our approach is rather robust for the transition-metal-containing systems.We will address the following questions in this paper: (i) What are the most likely candidates for the $\mathbf{H_{ox}^{air}}$, $\mathbf{H_{ox}}$, and $\mathbf{H_{red}}$? (ii) What do the electronic structures of these redox states tell us? (iii) What role does the bridging CO play in catalytic reactions?

From our calculations, we found that (i) the 2Fe subunit in the $\mathbf{H_{ox}^{air}}$ is mostly likely to be a *Fe(II)−Fe(II) complex with a hydroxyl (OH^-) group bonded at the Fe^d*, (ii) a *Fe(II)−Fe(I)* complex is the best candidate for the 2Fe subunit in the $\mathbf{H_{ox}}$, which is consistent with the results of Cao and Hall,[20] and (iii) the 2Fe subunit in the $\mathbf{H_{red}}$ is a mixture[13] with the major component probably being a protonated *Fe(I)−Fe(I)* complex.

(17) De Lacey, A. L.; Stadler, C.; Cavazza, C.; Hatchikian, E. C.; Fernandez, V. M. *J. Am. Chem. Soc.* **2000**, *122*, 11232.
(18) Nicolet, Y.; De Lacey, A. L.; Vernede, X.; Fernandez, V. M.; Hatchikian, E. C.; Fontecilla-Camps, J. C. *J. Am. Chem. Soc.* **2001**, *123*, 1596.
(19) Mortenson, L. E.; Chen, J.-S. *Biochim. Biophys. Acta* **1980**, *594*, 105.
(20) Cao, Z. X.; Hall M. B. *J. Am. Chem. Soc.* **2001**, *123*, 3734.
(21) Fan, H.-J.; Hall, M. B. *J. Am. Chem. Soc.* **2001**, *123*, 3828.
(22) Dance, I. *Chem. Commun.* **1999**, *17*, 1655.

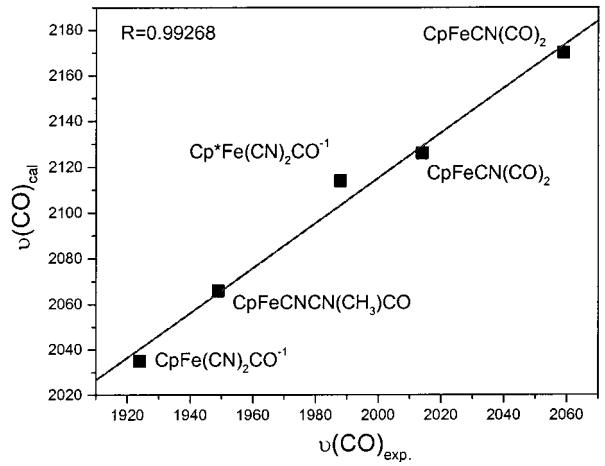

Figure 2. Linear fitting of the calculated CO stretching frequencies, $\upsilon(CO)_{calcd}$, against the experimental data, $\upsilon(CO)_{expt}$. The experimental data from the model complexes used in this figure could be found in the ref 30, 31.

The electronic structures of the redox states have been analyzed. We also found that the presence of the CO_b is crucial to stabilize the low-oxidation states of the 2Fe subunit.

The remainder of the paper is outlined as follows. Our calculation methods are described in section 2. In section 3, we first characterize each redox state by comparing our calculated candidates with all the experimental data. Then, we discuss the chemistry in each assigned redox state. Following this, the results of our electronic structure analysis of the 2Fe subunit will be presented. In section 4, conclusions are outlined.

2. Calculation Methods

Density functional theory calculations with a generalized gradient approximation[23] have been utilized. The program used is CASTEP.[24] The electronic wave functions were expanded in a plane wave basis set, and the ionic cores were described by ultrasoft pseudopotentials.[25] For the ultrasoft pseudopotential of Fe, the nonlinear core correction (NLCC) is included. The vacuum region between molecules was 10 Å, and a cutoff energy of 380 eV was used. A convergence check has been performed by increasing the vacuum region to 12 Å, and the cutoff energy, to 450 eV (the difference in the geometry is found to be below 0.001 Å, and the relative total energy is below 0.4 meV/atom). The accuracy of this method has been demonstrated previously.[26−28]

In this work, CO stretching frequencies of the 2Fe subunit were calculated.[29] To evaluate the systematic error in the calculated CO stretching frequencies in an Fe−CO bonding environment, we have optimized the structures of several model complexes, $CpFe(CN)_2CO^-$, $CpFe(CN)(CNCH_3)CO$, $CpFe(CN)CO)_2$, and $Cp^*Fe(CN)2(CO)^-$ (these complexes have been synthesized, and their FTIR spectra have been studied by Darensbourg et al. in detail[30,31]). In Figure 2, we show that there is a good linear relationship between the calculated CO frequencies and the experimental data ($R = 0.99$). The calculated values are generally larger by 115 ± 10 cm^{-1}. To avoid this systematic error, we subtracted 115 cm^{-1} from the calculated CO vibrational frequency, and the result is taken as the predicted value hereafter. It should be mentioned that the stretching frequencies of two terminal CN^- ligands were also measured experimentally. However, considering that their frequencies vary in a trend similar to that of terminal CO but to a lesser extent,[17,18,30,31] they will not be discussed in this paper.

3. Results and Discussion

3.1. Chemical Model for the 2Fe Subunit. As mentioned in the Introduction, there are two subunits in the catalytic center (the H-cluster) of Fe-only hydrogenases: (i) a novel 2Fe subunit and (ii) a regular [4Fe−4S] cubane. A general consensus is that the [4Fe−4S] cluster is redox-inactive during the catalytic cycle[10,11,16] and that it is the 2Fe subunit that determines the redox reactivity of the H-cluster. To obtain the best compromise with respect to the computational cost, we used the following complex, $[(H(CH_3)S)(CO)(CN^-)Fe^p(\mu\text{-DTN})(\mu\text{-CO})Fe^d(CO)(CN^-)(L)]^z$ (z is the net charge in the complex; Fe^p = the proximal Fe; Fe^d = the distal Fe; L is the ligand that bonds with the Fe^d at the trans position to the CO_b) to model the 2Fe subunit, illustrated in Figure 1b. In this model, two points should be noted. First, the [4Fe−4S] cubane was truncated and replaced by a H atom, and thus the cysteine-S ligand at the Fe^p was represented by a $S(CH_3)H$. Second, the two bridging thiolate groups were modeled by a $-SCH_2NHCH_2S-$ (DTN) chain, as suggested by Nicolet et al.[18] for DdH. This model is similar to the one used by Cao and Hall, except that a PDT chain which links two Fe ions was utilized in their model (hereafter our model will be referred as the (μ-DTN) model, and the model used by Cao and Hall as the (μ-PDT) model).

3.2. Assignment of the Redox States of the 2Fe Subunit. Oxidized, Active State (H_{ox}). Many different redox states were calculated, and it was found that the best candidate for the $\mathbf{H_{ox}}$ is complex **1** (see Figure 3), Fe(II)−Fe(I)(vacant) (the label of (vacant) means that the position trans to the CO_b of the Fe^d is vacant, the same meaning hereafter). The properties of optimized complex **1** agree well with all the available experimental data. First, the Fe(II)−Fe(I)(vacant) **1** is a spin-polarized complex with $S = {}^1/_2$, and our Mulliken analysis shows that the spin densities are largely localized on the Fe^d. This result is consistent with the EPR observation (the rhombic $g = 2.10$ signal[9−16]) and the previous theoretical calculation of Cao and Hall using (μ-PDT) model.[20] Second, the main structural parameters of the 2Fe subunit, namely the Fe−Fe distance (2.50 Å) and the Fe−S_b (bridging S) distance (average 2.29 Å), are very close to the reported crystal structure data of 2.6 and 2.3 Å, respectively (for DdH).[10,11] Third, the predicted CO frequencies of the Fe(II)−Fe(I)(vacant) **1**, $\upsilon(CO_{t1}) = 1947$, $\upsilon(CO_{t2}) = 1938$, and $\upsilon(CO_b) = 1828$ cm^{-1}, are very close to experimental values (1965, 1940, and 1802 cm^{-1} respectively[17]) (Table 1). Fourth, the H_2O could not bond to the Fe^d of **1**. The structural optimization of **1** with a H_2O close to the vacant site of the Fe^d yields structure **2** with only weak hydrogen bonding between the H_2O and the terminal CN^- of the Fe^d. This result is in line with the crystal structure for DdH;[11] The Fe^d is apparently five-coordinated with the position trans to the CO_b being vacant.

To further confirm the above assignment for the $\mathbf{H_{ox}}$, it is of significance to study the $\mathbf{H_{ox}}$-related complexes. Although H_2O

(23) Perdew, J. P.; Chevary, J. A.; Vosko, S. H.; Jackson, K. A.; Pederson, M. R.; Singh, D. J.; Fiolhais, C. *Phys. Rev. B.* **1992**, *46*, 6671.
(24) Payne, M. C.; Teter, M. P.; Allan, D. C.; Arias, T. A.; Joannopoulos, J. D. *Rev. Mod. Phys.* **1992**, *64*, 1045.
(25) Vanderbilt, D. *Phys. Rev. B*, **1990**, *41*, 7892.
(26) (a) Liu, Z.-P.; Hu, P. *J. Chem. Phys.* **2001**, *114*, 8244. (b) Liu, Z.-P.; Hu, P. *J. Am. Chem. Soc.* **2001**, *123*, 12596.
(27) (a) Zhang, C. J.; Hu, P. *J. Am. Chem. Soc.* **2001**, *123*, 1166. (b) Michaelides, A.; Hu, P. *J. Am. Chem. Soc.* **2000**, *122*, 9866. (c) Zhang, C. J.; Hu, P. *J. Am. Chem. Soc.* **2000**, *122*, 2134.
(28) (a) Liu Z.-P.; Hu, P.; Alavi A. *J. Chem. Phys.* **2001**, *114*, 5956. (b) Zhang, C. J.; Liu, Z.-P.; Hu, P. *J. Chem. Phys.* **2001**, *115*, 609.
(29) (a) Michaelides, A.; Hu P. *J. Am. Chem. Soc.* **2001**, *123*, 4235. (b) Michaelides, A.; Hu, P. *J. Chem. Phys.* **2001**, *114*, 513.
(30) Darensbourg, D. J.; Reibenspies, J. H.; Lai, C.-H.; Lee, W.-Z.; Darensbourg, M. Y. *J. Am. Chem. Soc.* **1997**, *119*, 7903.
(31) Lai, C.-H.; Lee, W.-Z.; Miller, M. L.; Reibenspies, J. H.; Darensbourg, D. J.; Darensbourg, M. Y. *J. Am. Chem. Soc.* **1998**, *120*, 10103.

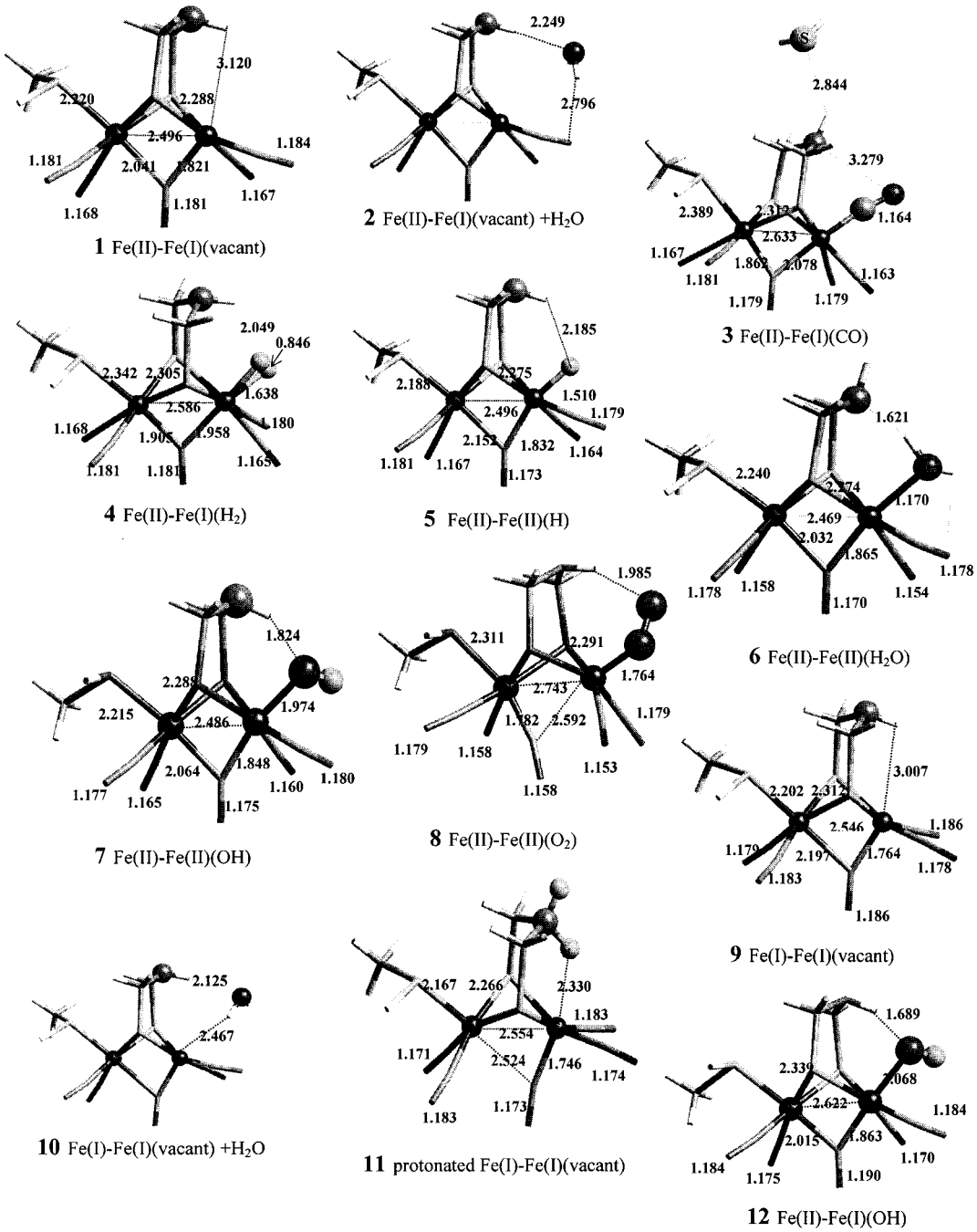

Figure 3. Optimized three-dimensional structures of redox states. Important atoms (e.g., the Fe atoms) are shown as balls, while others are shown as cylinders. For complex **3**, Fe(II)−Fe(I)(CO), a SH_2 group is placed near the N of DTN (see ref 38 for explanation). In each structure important distances (Å) are labeled (the $Fe-S_{bridging}$ bond distance labeled is the averaged one of all the four $Fe-S_{bridging}$ distances).

(electron donor) could not bond with the Fe^d in **1**, CO, H_2, and the H atom (electron acceptor) were found to be easily coordinated into the Fe^d, the optimized structures of which are labeled as **3**, **4**, and **5**, respectively. The fact that the Fe^d prefers to bond with the electron acceptor rather than the electron donor agrees with the low oxidation state in the 2Fe subunit. In agreement with the experimental observation,[4] the calculation results strongly suggest that the catalytic ability of the Fe(II)−Fe(I)(vacant) **1**, the $\mathbf{H_{ox}}$, can be inhibited by CO (the CO bonding energy with the 2Fe subunit was calculated to be 144 kJ/mol (1.49 eV)), while the H_2 molecule bonding with the $\mathbf{H_{ox}}$ is highly reversible (the H_2 binding at the Fe^d of **1** is found to be exothermic by 8.68 kJ/mol (0.09 eV)).

The CO-inhibited $\mathbf{H_{ox}}$ ($\mathbf{H_{ox}-CO}$) has been extensively studied experimentally and the results have been used to provide important insight into the reaction mechanism of Fe-only hydrogenases.[34−37] Comparison between experiments and calculations for the Fe(II)−Fe(I)(CO) **3** is therefore of interest.[38] Using photolysis, Peters and co-workers[37] showed that the major structure difference between the $\mathbf{H_{ox}}$ and the $\mathbf{H_{ox}-CO}$ is the

(32) Niu, S.; Thomson, L. M.; Hall. M. B. *J. Am. Chem. Soc.* **1999**, *121*, 4000.
(33) Amara, P.; Volbeda, A.; Fontecilla-Camps, J. C.; Field, M. J. *J. Am. Chem. Soc.* **1999**, *121*, 4468.
(34) Adams, M. W. W. *J. Biol. Chem.* **1987**, *262*, 15054.
(35) Kowal, A. T.; Adams, M. W. W.; Johonson, M. K. *J. Biol. Chem.* **1989**, *264*, 4342.
(36) Lemon B. J.; Peters J. W. *Biochemistry* **1999**, *38*, 12969.
(37) Lemon B. J.; Peters J. W. *J. Am. Chem. Soc.* **2000**, *122*, 3793.

Table 1. Predicted CO Stretching Frequencies ($\nu(CO)_{Pred.}$) of the Different Redox States[a]

species	$\nu(CO)_{pred.}$ (cm^{-1})	$\nu(CO)_{expt}$ (cm^{-1})
1 Fe(II)−Fe(I)(vacant)	1947, 1938, 1828	1965, 1940, 1802 (**H_{ox}**)
2 Fe(II)−Fe(I)(vacant) + H_2O	1956, 1947, 1805	
3 Fe(II)−Fe(I)(CO)	1988, 1974, 1947, 1840	2016, 1972, 1963, 1811 (**H_{ox}−CO**)
4 Fe(II)−Fe(I)(H_2)	1965, 1934, 1825	
5 Fe(II)−Fe(II)(H)	1978, 1946, 1893	1965, 1940, 1916, 1894 (**H_{red}**)
6 Fe(II)−Fe(II)(H_2O)	2072, 2036, 1921	
7 Fe(II)−Fe(II)(OH)	2007, 1968, 1867	2007, 1983, 1847 (**H_{ox}^{air}**)
8 Fe(II)−Fe(II)(O_2)	2072, 2032, 2029	
9 Fe(I)−Fe(I)(vacant)	1850, 1842, 1785	
10 Fe(I)−Fe(I)(vacant)+H_2O	1860, 1823, 1798	
11 protonated Fe(I)−Fe(I)(vacant)	1912, 1893, 1885	1965, 1940, 1916, 1894 (**H_{red}**)

[a] The experimental IR data ($\nu(CO)_{expt}$) for the **H_{ox}^{air}**, **H_{ox}**, **H_{red}**, and **H_{ox}−CO** are listed beside their best candidates. Each structure of calculated redox states is shown in Figure 3.

position variation of the CO_b in the 2Fe subunit: The main structure of **H_{ox}−CO** should remain similar to that of the **H_{ox}** except for the position of the bridging CO. This is indeed confirmed by our calculations (comparing the structure of **1** with **3**). The distance between the Fe^d and the CO_b was calculated to be 1.837 Å (expt: 1.85 Å) in the **H_{ox}** and 2.078 Å (expt: 2.09 Å) in the **H_{ox}−CO**, respectively, agreeing very well with experiment of Peters et al.[37] The predicted CO stretching frequencies of **3** (Table 1) are $\nu(CO_{t2})$ = 1988, 1974 (expt: 2016, 1972), $\nu(CO_{t1})$ = 1947 (expt: 1963), and $\nu(CO_b)$ = 1840 (expt: 1811) cm^{-1}, which also match reasonably with experimental data.[17] Importantly, the increase of bridging CO frequency from the **H_{ox}** to the **H_{oxi}−CO** was calculated to be 12 cm^{-1}, well reproducing the 9 cm^{-1} increase observed in the experiment.[17]

Fully Oxidized, Inactive State (H_{ox}^{air}). The fully oxidized (isolated in air) 2Fe subunit of Fe-only hydrogenases is inactive and EPR-silent, but can be activated by a reductive treatment. The FTIR spectrum of the **H_{ox}^{air}** shows three bands at 2007, 1983, 1847 cm^{-1} for the stretching frequencies of CO ligands.[15] With the **H_{ox}** being associated with the Fe(II)−Fe(I)(vacant) **1**, one would expect that the fully oxidized, inactive state is related to an Fe(II)−Fe(II) complex, such as the Fe(II)−Fe(II)(H_2O) **6**. Complex **6** is a nonspin-polarized state (consistent with the experiment in which the **H_{ox}^{air}** is EPR-silent), and the predicted CO vibrational frequencies are in better agreement with those of experiments compared to those of Fe(II)−Fe(I) and Fe(I)−Fe(I) complexes. However, the CO vibrational frequencies of the Fe(II)−Fe(II)(H_2O) **6** (2072, 2036, 1921 cm^{-1}) still appear too high compared to the experimental ones (2007, 1983, 1847 cm^{-1}).[15] Particularly, the predicated $\nu(CO_b)$ is 74 cm^{-1} higher than experiment one.

Alternative candidates for the **H_{ox}^{air}** may be Fe(II)−Fe(II)-(OH) and Fe(II)−Fe(II)(O_2), considering that OH^- and O_2 might be available as the enzyme is aerobically isolated. To verify this, we have optimized the structures of Fe(II)−Fe(II)(OH) **7** and Fe(II)−Fe(II)(O_2) **8**. Their vibrational frequencies are calculated and also listed in Table 1. It is clear that the predicted ν(CO) of Fe(II)−Fe(II)(OH) **7** match the experimental values very well (the differences are within 20 cm^{-1}), while the predicted CO stretching frequencies of Fe(II)−Fe(II)(O_2) **8** (2072, 2032, 2029 cm^{-1}) are much higher than experimental values. In fact, in the optimized structure of complex **8** it is found that the CO_b significantly shifts toward the Fe^p, becoming terminal-like (Figure 2), which causes $\nu(CO_b)$ to be too high compared to the experimental value of 1847 cm^{-1}. In addition, the structure of complex **7** is also more consistent with the reported CpI crystal structures,[10] where a H_2O-like ligand, not a diatomic ligand, was suggested to bond with the Fe^d. Therefore, we assign the Fe(II)−Fe(II)(OH) as the **H_{ox}^{air}**.

Fully Reduced State (H_{red}). With the understanding of the oxidized states, the **H_{ox}** and the **H_{ox}^{air}**, the fully reduced state of the 2Fe subunit is thus mostly likely to be associated with Fe(I)−Fe(I) complexes, such as Fe(I)−Fe(I)(vacant) **9**. Complex **9** is, as optimized, a nonspin-polarized state, which agrees with the EPR-silent observation for the **H_{red}**. With a H_2O at the vacant site of complex **9**, structural optimization leads to structure **10**, in which H_2O could not bond with the Fe^d. This is also consistent with the experimental observations; for the **H_{red}** of DdH the Fe^d is only five-coordinated.[18] However, by closer examination of the structure of **9**, two major difficulties were encountered when we tried to reconcile the calculated values of Fe(I)−Fe(I)(vacant) **9** with the experimental values for the reduced form of DdH. First, the CO_b in complex **9** is not in the correct position. The calculated distances of the C−Fe^d and the C−Fe^p in the Fe(I)−Fe(I)(vacant) **9** are 1.764 and 2.179 Å respectively, which are quite different from the experimental values (1.69, 2.4/2.56 Å[18] or 1.8, 2.6 Å[11]). Second, the optimized CO_b bond length of **9** appears too long, which is even longer than 1.181 Å of the CO_b in the Fe(II)−Fe(I)(vacant) **1**. Consequently, in the Fe(I)−Fe(I)(vacant) **9** the CO_b stretching frequency is even lower than 1802 cm^{-1} ($\nu(CO_b)$ in the **H_{ox}**). This is contradictory to the experiment; in the **H_{red}**, the lowest CO-stretching frequency is at 1894 cm^{-1}, much higher than 1802 cm^{-1} in the **H_{ox}**.

Nevertheless, the above inconsistency can be understood as follows. Compared to the Fe(II)−Fe(I)(vacant) **1**, the **H_{ox}**, the Fe(I)−Fe(I)(vacant) **9** accumulates more negative charges in the 2Fe subunit center. From our calculations we found that the extra negative charges are mainly located near the CO_b (see section 3.4), which results in the CO_b 2π-antibonding orbital being partially occupied. This leads to a longer CO_b bond distance and a softer CO_b vibrational mode. Therefore, we speculated that the fully reduced state might be a protonated Fe(I)−Fe(I)(vacant) complex on the basis of the following two reasons: (i) the Fe(I)−Fe(I)(vacant) **9** might readily attract a proton because the N of the DTN is a base, and (ii) the

(38) For the Fe(II)−Fe(I)(CO), we found that the NH at the DTN tends to electrostatically interact with the exogenous CO (N−H- - -OC), which will soft the stretching mode of the CO_{exo} by about 30 cm^{-1}. To avoid this interaction, we added a SH_2 near the NH of the DTN forming H-bonding (H_2S- - -HN), as shown in Figure 3. This modelling is consistent with the experimental crystal structures,[11,18,39] and the optimised structure and the predicted CO frequencies provide a good match with the experimental data (see text). It should be mentioned that for other calculated structures the presence of the SH_2 group near the DTN linker has almost no effect on the vibrational frequencies of other CO since no direct H-bonding between SH_2 and other CO ligands exist. In addition, we have also checked the H-bonding effect by putting H_2O molecules nearby the bridging CO or terminal CN^- ligands, which models the H-bonding of 2Fe subunit with the protein environment: we found that there is almost no change in the main structure of 2Fe subunit, and the CO stretching frequencies will be slightly affected by about 10−20 cm^{-1}.

protonated Fe(I)−Fe(I)(vacant) is an intermediate in the catalytic cycle (see section 3.3), and thus it is chemically meaningful.

The protonated Fe(I)−Fe(I)(vacant) **11**, in which a proton is attached at the N of the DTN, was optimized, and its structure indeed agrees well with the reduced form of DdH reported recently.[18] The CO_b is at a bridge-to-terminal position with the bond distances of C−Fe^d and C−Fe^p being 1.745 Å (expt: 1.69 Å[18] or 1.8 Å[11]) and 2.524 Å (expt: 2.4/2.56 Å[18] or 2.6 Å[11]), respectively. The CO stretching frequencies of **11** are 1912 ($\upsilon(CO_{t1})$), 1894 ($\upsilon(CO_b)$), and 1885 ($\upsilon(CO_{t2})$) cm^{-1}, which are remarkably consistent with the experimental ones (1916 and 1894 cm^{-1}) for the $\mathbf{H_{red}}$.[15,18] It is interesting to notice that the predicted $\upsilon(CO_b)$ and $\upsilon(CO_{t2})$ are very close (9 cm^{-1} difference).

It should be mentioned that the FTIR spectrum of the $\mathbf{H_{red}}$ exhibits one major CO band at 1894 cm^{-1} as well as other minor bands (1941 and 1965 cm^{-1}). Pierik et al.[15] suggested, therefore, that the $\mathbf{H_{red}}$ might be a mixture of different states. We expect that the protonated Fe(I)−Fe(I)(vacant) **11** may be the main component of this mixture. We further suggest that the Fe(II)−Fe(II)(H) **5**, might be another component in the $\mathbf{H_{red}}$ mixture on the basis of the following reasons. First, the calculated CO stretching frequencies of complex **5** match the minor IR bands observed in the $\mathbf{H_{red}}$: $\upsilon(CO_{t1}) = 1946$ cm^{-1} (expt: 1941), $\upsilon(CO_{t2}) = 1978$ cm^{-1} (expt: 1965) and $\upsilon(CO_b) = 1893$ cm^{-1} (expt: 1893). Second, complex **5** is a nonspin-polarized state, which is also consistent with experiment. Third, complex **5** is a self-arranged form of **11** with a low barrier.[40] Therefore, we expect that some of complex **5** might always coexist with **11** under the experimental conditions. Interestingly, complex **5** also possesses a CO_b vibrational frequency at 1893 cm^{-1} which is very similar to that of $\upsilon(CO_b)$ and $\upsilon(CO_{t2})$ in complex **11**. Therefore, these frequencies may overlap with each other and this may explain the high intensity of 1894 cm^{-1} band in the FTIR spectrum.[15,18]

3.3. Discussion on the Assignment of the Redox States. Perhaps the most important criterion for an assignment of the redox states is whether it makes chemical sense. In addition to the structural agreement, here we will discuss the chemistry of each redox state we have assigned. As will be discussed below (section 3.4), any state with an oxidation state higher than Fe(II)−Fe(II) is not stable. Therefore, the fully oxidized state, the $\mathbf{H_{ox}^{air}}$, is most likely to be associated with the Fe(II)−Fe(II) derived complexes. DFT calculations on the (μ-PDT) model for the 2Fe subunit by Cao and Hall[20] suggested that Fe(II)−Fe(II)(vacant) and Fe(II)−Fe(II)(H_2O) are possible candidates. In our (μ-DTN) model the Fe(II)−Fe(II)(vacant) complex is unstable, the structural optimization of which will lead to a largely distorted geometry with the N in the DTN being pivoted to the Fe^d. This is apparently owing to the strong electrostatic attraction between the N (negative charge) and the Fe^d (positive charge). Therefore, we ruled out the possibility of the Fe(II)−Fe(II)(vacant) as a candidate for the $\mathbf{H_{ox}^{air}}$ in DdH.

Three Fe(II)−Fe(II) derived complexes are stable from our calculations: the Fe(II)−Fe(II)(H_2O) **6**, the Fe(II)−Fe(II)(OH) **7**, and the Fe(II)−Fe(II)(O_2) **8**. It is possible for all three of these complexes to be formed during the aerobic isolation of the Fe-only enzyme. The Fe(II)−Fe(II)(O_2) **8** can be first ruled out because of its CO stretching frequencies are too high and its structures are quite different from the experimental ones, as mentioned above. In addition to the fact that the CO-stretching frequencies of the Fe(II)−Fe(II)(OH) **7** match better with the experimental value than those of **6**, the gradual reductive titration experiment of $\mathbf{H_{ox}^{air}}$ also seems to favor the assignment of Fe(II)−Fe(II)(OH) as the $\mathbf{H_{ox}^{air}}$; it was found that in the course of a gradual reductive titration starting from the $\mathbf{H_{ox}^{air}}$, a transient 2.06 rhombic signal was detected by EPR, which is assigned as a partially reduced and inactive state.[12−13] As shown in Figure 4 (dotted line), the reductive titration involved with the Fe(II)−Fe(II)(OH) **7** being the $\mathbf{H_{ox}^{air}}$ may indeed yield a *spin-polarized* state Fe(II)−Fe(I)(OH) **12** (the structure of Fe(II)−Fe(I)(OH) is optimized and shown in Figure 3). However, a reductive treatment starting from the Fe(II)−Fe(II)(H_2O) will not yield any partially reduced, inactive intermediate state.

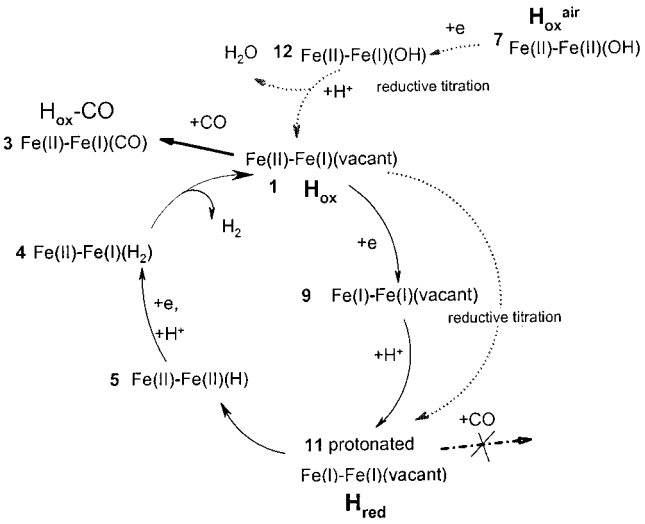

Figure 4. Schematic diagram for the redox states change during H_2 metabolism, and the reductive titration.

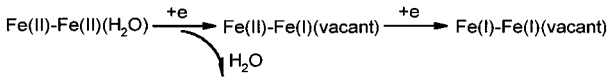

Therefore, we argue that the Fe(II)−Fe(II)(OH) is a better candidate for the $\mathbf{H_{ox}^{air}}$.

Compared with other redox states, the uncertainty that in the $\mathbf{H_{ox}}$ the 2Fe subunit is the Fe(II)−Fe(I)(vacant) is even smaller. Both our model and the previous (μ-PDT) model of Cao and Hall match nicely with the experimental data of the $\mathbf{H_{ox}}$. Moreover, our calculations also show that exogenous CO can indeed inhibit the $\mathbf{H_{ox}}$ with a strong binding energy, while H_2 bonding at the Fe^d of the $\mathbf{H_{ox}}$ is highly reversible.

Once the $\mathbf{H_{ox}^{air}}$ and the $\mathbf{H_{ox}}$ are assigned, the fully reduced state, the $\mathbf{H_{red}}$, can be readily assigned as Fe(I)−Fe(I) derived complexes. Using the (μ-PDT) model Cao and Hall suggested that the $\mathbf{H_{red}}$ may be an Fe(I)−Fe(I)(vacant) complex, in which the CO_b shifts to the Fe^d and becomes a terminal one. In our calculations we found that the optimized structure of the protonated Fe(I)−Fe(I) (vacant) **11** is more consistent with the recent experimental finding for the $\mathbf{H_{red}}$; the bridging CO shifts toward the Fe^d (at a bridge-to-terminal position), but it is by no means a terminal CO. Complex **11** is also an intermediate in the catalytic H_2 production, as shown in Figure 4 (solid arrow line).

(39) Bennett, B.; Lemon, B. J.; Peters, J. W. *Biochemistry* **2000**, *39*, 7455−7460.
(40) Liu, Z.-P.; Hu, P. Unpublished results

Interestingly, it was found experimentally[39] that the incubation of the $\mathbf{H_{red}}$ under CO always results in the $\mathbf{H_{ox}-CO}$ rather than the $\mathbf{H_{red}-CO}$, with the concomitant H_2 production at the expense of reductive agents. It was suggested that CO either could not bond with the $\mathbf{H_{red}}$ or could highly reversibly bond with the $\mathbf{H_{red}}$, which could not compete with the catalytic H_2 production process. In line with this experimental observation, our calculations showed that the fully reduced form, such as the Fe(I)−Fe(I)(vacant) **9** and the protonated Fe(I)−Fe(I)-(vacant) **11** could not bond with an exogenous CO; when the CO was placed very close to the Fe^d, a structure optimization yielded a structure in which the bond between the cysteine-S and the Fe^p is broken; if the CO was put at a reasonable distance, say 2.5 Å, away from the Fe^d, it was found that there are repulsive forces between the CO and the Fe^d and that a consequent structural optimization would result in a structure in which there is no bond between the CO and the Fe^d. Considering that in the CO-inhibiting process, it is always the CO that approaches the 2Fe subunit, we can conclude that exogenous CO cannot bond with the $\mathbf{H_{red}}$, as shown in Figure 4.

It is worth mentioning that there are similarities as well as significant differences between the (μ-DTN) model used in our work and the (μ-PDT) model[20] utilized by Cao and Hall. From our calculations, we found that the N (or NH) of DTN will directly interact with the Fe^d (an electrostatic interaction), which is lacking in the case of the μ-PDT complexes. For states, in which such direct electrostatic interaction is weak, both models should give rise to similar results. For example, for the Fe(II)−Fe(I)(vacant) (complex **1**), both models yielded similar structures. For states where such interaction is strong, results from these two models should be very different. An obvious example is the Fe(II)−Fe(II)(vacant) species that is stable in the (μ-PDT) model[20] and unstable in the (μ-DTN) model mentioned above. Another very important difference between these two models is that the DTN ligand can significantly facilitate molecular H_2 production due to the presence of a built-in base.[40]

3.4. Electronic Structure of the 2Fe Subunit. Once we have a sound base for the redox states, we are in a position to explore the electronic structure in these systems. It is generally known in inorganic chemistry that the most common Fe oxidation states are Fe(II) or Fe(III), while Fe(I) complexes are usually unstable. This is due to the fact that the Fe 3d valence electrons prefer the $3d^5$ (half occupied) or $3d^6$ (t_{2g} states occupied) configurations. However, our total energy calculations show that Fe(I)−Fe(I) species are the most stable complexes in the 2Fe subunit, which is consistent with the suggestions from recent synthetic work.[41−45] In addition, both Hall's group and ours have assigned the highest oxidation state as Fe(II)−Fe(II), and the lowest, as Fe(I)−Fe(I). Therefore, one of the most important questions concerning the reactivity of Fe-only hydrogenases is why the low oxidation states, such as Fe(I)−Fe(I), are stable while the high oxidation states, for example Fe(III)−Fe(III) and Fe(III)−Fe(II), do not exist.

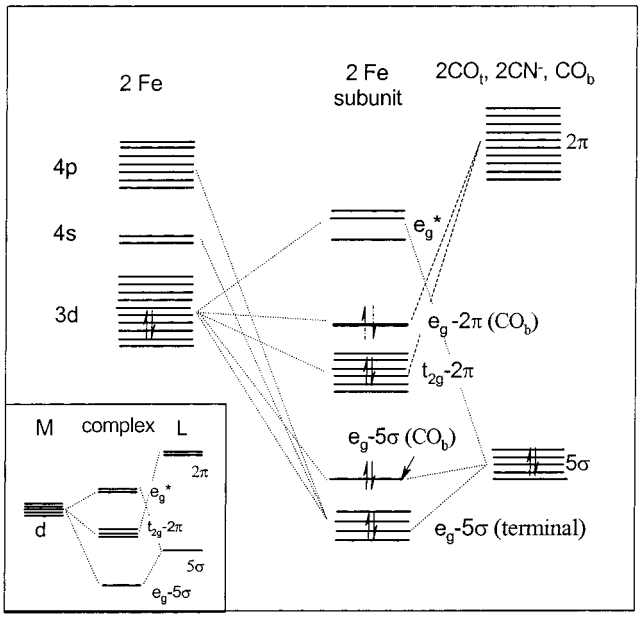

Figure 5. Molecular orbital diagram for the 2Fe subunit. The insert shows a typical metal d orbital splitting induced by strong ligands, such as CO, for an octahedral complex (simplified).[46]

We have examined the electronic structures in our calculated systems, the result of which can be briefly described as follows. Figure 5 is the interaction diagram between the Fe valence orbitals (3d, 4s, 4p) and the 5σ, 2π orbitals of CO and CN^- ligands (the interaction between the Fe valence orbitals and the S 2p orbital is less important in terms of understanding of reactivity of the 2Fe subunit and is thus omitted here). The energy levels of the 2Fe subunit are shown in the middle. It was found that all the redox states (Fe(II)−Fe(II), Fe(II)−Fe(I), and Fe(I)−Fe(I)) are very similar except for the occupation of a frontier orbital, labeled as $e_g-2\pi$ in Figure 5. It is unoccupied in Fe(II)−Fe(II), half-occupied in Fe(II)−Fe(I), and fully occupied in Fe(I)−Fe(I). According to the orbital symmetry,[46] important molecular orbitals in the 2Fe subunit can be divided into four groups, each being mixing states of (i) strong 5σ orbital of terminal CN^-, CO_t ligands and weak Fe e_g ($d_{x^2-y^2}$, d_{z^2}) orbital (strong σ bonding states); (ii) very strong 5σ orbital of CO_b ligand and weak Fe e_g (d_{z^2}) orbital (weak σ bonding state); (iii) strong Fe t_{2g} (d_{xy}, d_{yz}, d_{xz}) orbital and weak 2π orbtial of ligands (strong π bonding state); and (iv) strong Fe e_g (d_{z^2}) orbital and 2π orbital of CO_b (weak π bonding state), labeled as $e_g-5\sigma$ (terminal), $e_g-5\sigma$ (CO_b), $t_{2g}-2\pi$ and $e_g-2\pi$ (CO_b), respectively. The novel feature here is that the $e_g-2\pi$ orbital is a bonding orbital between the CO_b and the Fe^d. Thus, the electron occupation of this orbital will stabilize the system. This explains why the Fe(I)−Fe(I) complex (the $e_g-2\pi$ orbital is fully occupied) is stable. We also noted that to obtain Fe(III)−Fe(III) and Fe(III)−Fe(II) states, electrons in even stronger bonding orbitals of $t_{2g}-2\pi$ must be depleted, which is strongly energetically disfavored. This may be the reason why Fe(III)−Fe(III) or Fe(III)−Fe(II) species do not exist in the catalytic cycle.

Naturally, one would ask why the energy level of the $e_g-2\pi$ orbital is so low (being a bonding state). Usually, this state

(41) Razavet, M.; Davies S. C.; Hughes, D. L.; Pickett, C. J. *Chem. Commun.* **2001**, *9*, 847.
(42) Lyon E. J.; Georgakaki, I. P.; Reibenspies J. H.; Darensbourg M. Y. *J. Am. Chem. Soc.* **2001**, *123*, 3268.
(43) Lyon, E. J.; Georgakaki, I. P.; Reibenspies J. H.; Darensbourg, M. Y. *Angew. Chem., Int. Ed.* **1999**, *38*, 3178.
(44) Schmidt, M.; Contakes, S. M.; Rauchfuss, T. B. *J. Am. Chem. Soc.* **1999**, *121*, 9736.
(45) Le Cloirec, A.; Best, S. P.; Borg, S.; Davies, S. C.; Evans, D. J.; Hughes, D. L.; Pickett, C. J. *Chem. Commun.* **1999**, *22*, 2285.
(46) Elschenbroich, C. H.; Salzer, A. *Organometallics: A Concise Introduction*; VCH: Weinheim, New York, Basel, Cambridge, 1992; p 188.

should be at an energy level similar to that of other e_g antibonding orbitals[46] (Figure 5 insert). We found that the CO_b plays an important role in lowering the energy level of $e_g-2\pi$ orbital. First, due to the bridging geometry the 5σ orbital of CO_b only weakly mixes with the Fe e_g orbital, compared to the 5σ orbitals of terminal CO and CN^- ligands. This leads to a splitting between one of the e_g and the t_{2g} orbitals smaller than the splitting of the other e_g with the t_{2g} orbitals caused by terminal ligands. Second, the e_g orbital can further interact with the 2π orbital of the CO_b, resulting in a formation of $e_g-2\pi$ bonding orbital with a further reduction in the energy level.

It is worth mentioning that in the $e_g-2\pi$ orbital more charge accumulates between the CO_b and the Fe^d than between the CO_b and the Fe^p. This indicates that the occupation in this orbital will mainly strengthen the bonding between the CO_b and the Fe^d. This is consistent with the experiments and also the calculated geometry trend, which shows that upon reduction (the occupation increase of the $e_g-2\pi$ orbital) the CO_b shifts toward the Fe^d.

4. Conclusions

With extensive DFT calculations and a thorough comparison with experiments, this work provides a detailed theoretical characterization of the redox states of the 2Fe subunit in Fe-only hydrogenases. A deeper understanding of the redox states has been obtained. In particular, we have gained some insight into the electronic structure of the redox states. Our results are as follows: (1) The 2Fe subunit in the $\mathbf{H_{ox}^{air}}$ is likely to be an Fe(II)−Fe(II)(OH). (2) The 2Fe subunit in the $\mathbf{H_{ox}}$ is identified to be an Fe(II)−Fe(I)(vacant). Exogenous CO can indeed bond strongly with the Fe(II)−Fe(I) complex (*CO inhibition*), while H_2 molecule bonding to this complex is highly reversible. (3) The 2Fe subunit in the $\mathbf{H_{red}}$ is a mixture, with the major component being a protonated Fe(I)−Fe(I) complex. This protonated complex is most likely to mix with its self-arranged form, Fe(II)−Fe(II) hydride. Exogenous CO cannot bond with the Fe^d in the Fe(I)−Fe(I) species.

By detailed analyses of the electronic structure of 2Fe subunit, we find that the major difference among all the redox states lies in the occupation of a frontier orbital, which is the mixing state between the Fe e_g and the CO_b 2π ($e_g-2\pi$ orbital). It is unoccupied in the $\mathbf{H_{ox}^{air}}$, half-occupied in the $\mathbf{H_{ox}}$, and fully occupied in the $\mathbf{H_{red}}$. The properties of this $e_g-2\pi$ orbital that determine the reactivity of 2Fe subunit are summarized as follows:

1. The $e_g-2\pi$ orbital is a bonding state (mainly between the Fe^d and the CO_b), which results in the preference of the 2Fe subunit to be low oxidation states, such as Fe(I)−Fe(I). To achieve high oxidation states, such as Fe(III)−Fe(III) or Fe(III)−Fe(II), electrons must be depleted in the $t_{2g}-2\pi$ orbitals that are even more stable than the $e_g-2\pi$ orbital, which will lead to energetically disfavored electronic structures.

2. As the occupation in the $e_g-2\pi$ orbital increases, the bonding between the CO_b and the Fe^d is enhanced, which leads to the CO_b shifting toward the Fe^d upon the reduction of Fe-only hydrogenases, as observed experimentally.

Acknowledgment. We gratefully acknowledge the UKCP for computing time in T3E and the supercomputing center in Ireland for computing time in IBM-SP.

JA0118690